Modified mRNA directs the fate of heart progenitor cells and induces vascular regeneration after myocardial infarction

Lior Zangi[1–5,14], Kathy O Lui[1,2,6,14], Alexander von Gise[3,5], Qing Ma[3,5], Wataru Ebina[1,4], Leon M Ptaszek[1,2,7], Daniela Später[1,2], Huansheng Xu[1,2,6], Mohammadsharif Tabebordbar[1,8], Rostic Gorbatov[9], Brena Sena[9], Matthias Nahrendorf[9], David M Briscoe[10], Ronald A Li[6,11], Amy J Wagers[1,12], Derrick J Rossi[1,4], William T Pu[3,5] & Kenneth R Chien[1,2,13]

© 2013 Nature America, Inc. All rights reserved.

In a cell-free approach to regenerative therapeutics, transient application of paracrine factors *in vivo* could be used to alter the behavior and fate of progenitor cells to achieve sustained clinical benefits. Here we show that intramyocardial injection of synthetic modified RNA (modRNA) encoding human vascular endothelial growth factor-A (VEGF-A) results in the expansion and directed differentiation of endogenous heart progenitors in a mouse myocardial infarction model. VEGF-A modRNA markedly improved heart function and enhanced long-term survival of recipients. This improvement was in part due to mobilization of epicardial progenitor cells and redirection of their differentiation toward cardiovascular cell types. Direct *in vivo* comparison with DNA vectors and temporal control with VEGF inhibitors revealed the greatly increased efficacy of pulse-like delivery of VEGF-A. Our results suggest that modRNA is a versatile approach for expressing paracrine factors as cell fate switches to control progenitor cell fate and thereby enhance long-term organ repair.

Myocardial infarction in a human causes the death of billions of cardiomyocytes. The heart's limited capacity to regenerate these lost cardiomyocytes leads to compromised cardiac function and high morbidity and mortality. As a result, there has been intense interest in developing treatments to reduce or reverse myocardial injury. A number of strategies have been proposed for regenerative cardiovascular therapeutics, including transplantation of cells expanded *ex vivo*, delivery of therapeutic genes on naked DNA plasmids or viral vectors, and administration of recombinant proteins. Thus far, these approaches have had mixed results. Cell-based therapies have shown limited long-term engraftment and low efficacy. Gene-based methods have been hampered by poor control of dosage and duration, low gene-transfer efficiency, risk of genomic integration and associated tumorigenesis, and antiviral immune responses. Recombinant-protein approaches have been characterized by fleeting protein half-lives, poor targeting to the heart and complications due to systemic release. modRNA, in which one or more nucleotides is replaced by modified nucleotides, represents a potential alternative. Previous work has shown that modRNA mediates highly efficient, transient protein expression *in vitro* and *in vivo* without eliciting an innate immune response[1–6]. We therefore hypothesized that modRNA might provide an effective means to control the spatial and temporal delivery of gene products to enhance tissue repair or regeneration after injury.

The fetal and post-natal mammalian heart contains a diverse set of endogenous cardiovascular progenitors[7–17], but native expansion, mobilization and differentiation of progenitors *in vivo* are inadequate to restore myocardial function after injury[18], and inducing these processes for therapeutic benefit has proved difficult. Paracrine factors play key roles in regulating progenitor cell activity in heart development, and recent studies have likewise implicated paracrine factors in promoting cardiac repair and regeneration after myocardial infarction in experimental model systems[14,16,19]. In part, paracrine factors promote heart regeneration by stimulating the cardiomyogenic activity of poorly defined endogenous heart progenitors[14,19,20]. Given that native paracrine signals are often transient and precisely regulated in time and space, we further hypothesized that the pulse-like expression profile of modRNA might be well suited to delivering paracrine-factor

[1]Department of Stem Cell and Regenerative Biology, Harvard University, Cambridge, Massachusetts, USA. [2]Cardiovascular Research Center, Massachusetts General Hospital, Boston, Massachusetts, USA. [3]Department of Cardiology, Children's Hospital Boston, Boston, Massachusetts, USA. [4]Immune Disease Institute and Program in Cellular and Molecular Medicine, Children's Hospital Boston, Boston, Massachusetts, USA. [5]Boston and Harvard Stem Cell Institute, Cambridge, Massachusetts, USA. [6]Stem Cell & Regenerative Medicine Consortium, LKS Faculty of Medicine, University of Hong Kong, Pokfulam, Hong Kong. [7]Cardiac Arrhythmia Service, Massachusetts General Hospital, Boston, Massachusetts, USA. [8]Biological and Biomedical Sciences Program, Harvard Medical School, Boston, Massachusetts, USA. [9]Center for Systems Biology, Massachusetts General Hospital and Harvard Medical School, Boston, Massachusetts, USA. [10]Division of Nephrology, Children's Hospital Boston, Boston, Massachusetts, USA. [11]Cardiovascular Research Center, Mount Sinai School of Medicine, New York, New York, USA. [12]Howard Hughes Medical Institute, Cambridge, Massachusetts, USA. [13]Department of Cell and Molecular Biology and Medicine, Karolinska Institutet, Stockholm, Sweden. [14]These authors contributed equally to this work. Correspondence for reagents and protocols should be addressed to K.R.C. (kenneth.chien@ki.se) and for mouse models to W.T.P. (wpu@enders.tch.harvard.edu).

Received 10 May; accepted 6 August; published online 8 September 2013; corrected before print 19 September 2013; doi:10.1038/nbt.2682

signals that modulate heart progenitor activity and thereby promote heart repair or regeneration.

To test these hypotheses, we studied the kinetics and efficacy of modRNA-mediated gene transfer in a mouse myocardial infarction model. Previous work has shown that epicardial heart progenitors are activated within 48 h after mouse myocardial infarction and are amplified in a thickened epicardial layer at the surface of the heart. However, these cells are not mobilized to enter the myocardium and differentiate toward cardiovascular lineages as they do in the fetal heart[13,15,21], but rather remain on the heart surface and differentiate largely into fibroblasts and myofibroblasts. For initial proof-of-concept experiments, we studied modRNA encoding the VEGF-A protein, a potent angiogenic factor. Based on its angiogenic activity, VEGF-A has been proposed as a therapeutic agent to improve myocardial outcome after ischemic injury (**Supplementary Appendix** and **Supplementary Tables 1** and **2**). Previous human and animal studies of delivery of VEGF-A after injury using naked DNA plasmids, recombinant proteins and engineered viruses showed limited efficacy after myocardial infarction, but these negative results may have been due to suboptimal delivery and/or antiviral immune responses[22–25]. Temporal and spatial control of VEGF-A expression is likely to be critical for its therapeutic efficacy, as two independent groups showed that prolonged exposure of normal muscle to VEGF-A caused excessive vascular permeability[26–28]. Furthermore, our recent work identified a novel role for VEGF-A as a cell fate switch for multipotent *ISL1*$^+$ human heart progenitors, driving their differentiation away from cardiac muscle and toward the endothelial lineage[29]. The potential activity of VEGF-A on endogenous cardiac progenitors has not been studied *in vivo* or in the context of myocardial injury.

Here we asked whether *in vivo* delivery of VEGF-A modRNA given at the time of epicardial progenitor activation after myocardial infarction would stimulate their mobilization or modulate their differentiation. We found that modRNA mediates 'pulse-like' expression of VEGF-A and is superior to plasmid DNA in reducing infarct size, enhancing myocardial perfusion and improving survival. In part, this effect was due to a previously unknown effect of VEGF-A on epicardial progenitors. VEGF-A modRNA amplified these progenitors, mobilized their migration into the myocardium and redirected their differentiation toward cardiovascular lineages. These results indicate that modRNA gene transfer drives *in vivo* heart progenitor cell fate to enhance cardiac repair.

RESULTS

Pulse-like kinetics of modRNA gene delivery to heart and skeletal muscle

We evaluated the suitability of modRNA for gene transfer to heart and skeletal muscle—tissues that have been historically difficult to transfect. Notably, modRNA transfected primary fetal human, neonatal mouse, and adult rat cardiomyocytes or adult mouse skeletal myotubes with high efficiency (89%, 72%, 68% and 100%, respectively; **Supplementary Fig. 1**) and minimal toxicity (~80% cell survival, comparable to transfection vehicle control). This high efficiency represents a 10- to 40-fold increase compared to typical transfection efficiencies attained using nonviral DNA–mediated transfection[22,30]. modRNA likewise mediated efficient protein production in cardiac cells *in vivo*. Direct, single, intramyocardial injection of luciferase (Luc) modRNA yielded a robust bioluminescent signal indicative of dose- and time-dependent luciferase protein expression localized to the injection site (**Fig. 1a–c**). Luc was immediately expressed and reached high levels after only 3 h, peaked at 18 h and returned to

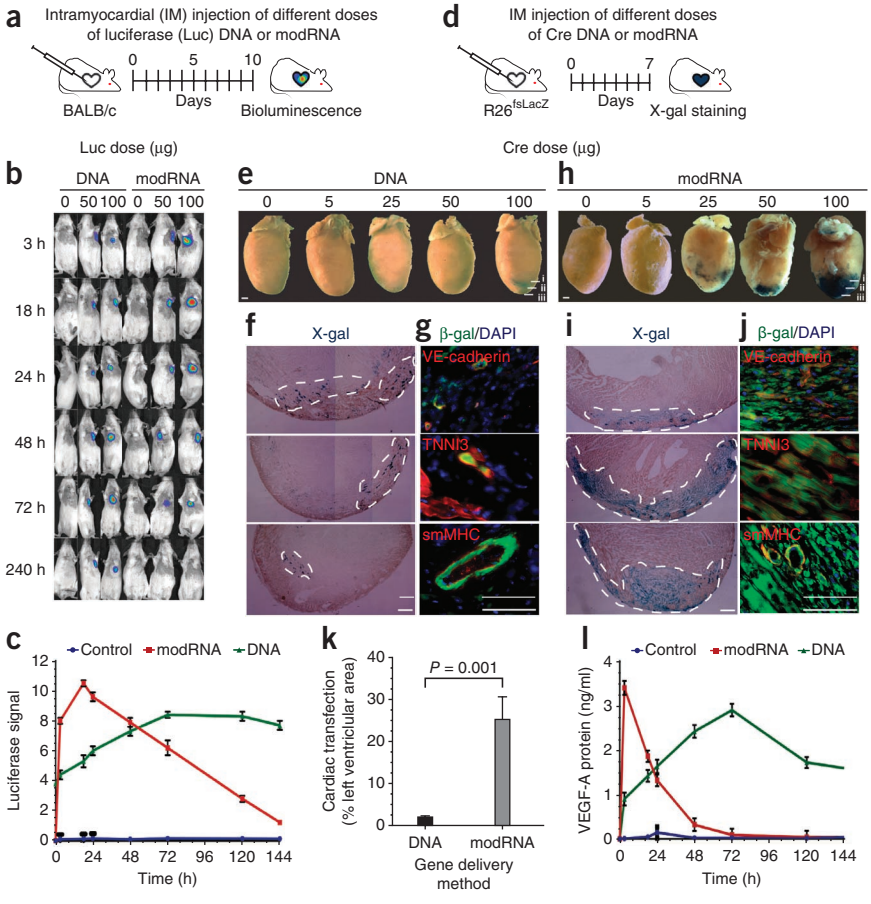

Figure 1 Highly efficient, transient gene transfer *in vivo* using modRNA. (**a**,**b**) Luciferase DNA or modRNA was delivered by myocardial injection (**a**). Protein expression was assayed by bioluminescence (**b**). (**c**) Time course of luciferase activity after injection of luciferase DNA or modRNA (100 μg) or vehicle only (control) per heart. (**d**) Cre DNA or modRNA, delivered by myocardial injection, catalyzed cardiac recombination, detected by X-gal staining (blue) for Cre-activated expression of LacZ from R26^{fsLacZ}. (**e**–**g**) Indicated doses of Cre DNA were injected intramyocardially into R26^{fsLacZ} hearts. DNA plasmid inefficiently transfected cells expressing endothelial, cardiomyocyte and smooth muscle lineage markers. Lines labeled i, ii and iii indicate planes of section in **f**. Scale bar, 400 μm (**e**) or 50 μm (**f**,**g**). (**h**–**j**) Indicated doses of Cre modRNA were injected intramyocardially into R26^{fsLacZ} hearts. modRNA efficiently transfected cells expressing endothelial, cardiomyocyte and smooth muscle lineage markers. Lines labeled i, ii and iii indicate planes of section in **i**. Scale bar, 400 μm (**h**) or 50 μm (**i**,**j**). (**k**) Summary of transfection efficiency of single 100 μg DNA or modRNA injection into cardiac muscle (left ventricle). (**l**) Kinetics of VEGFA modRNA expression in cardiac cells cultured *in vitro*. For **a**–**l**, $n = 3$, representative of two independent experiments. Error bars (**c**,**l**), s.d.

© 2013 Nature America, Inc. All rights reserved.

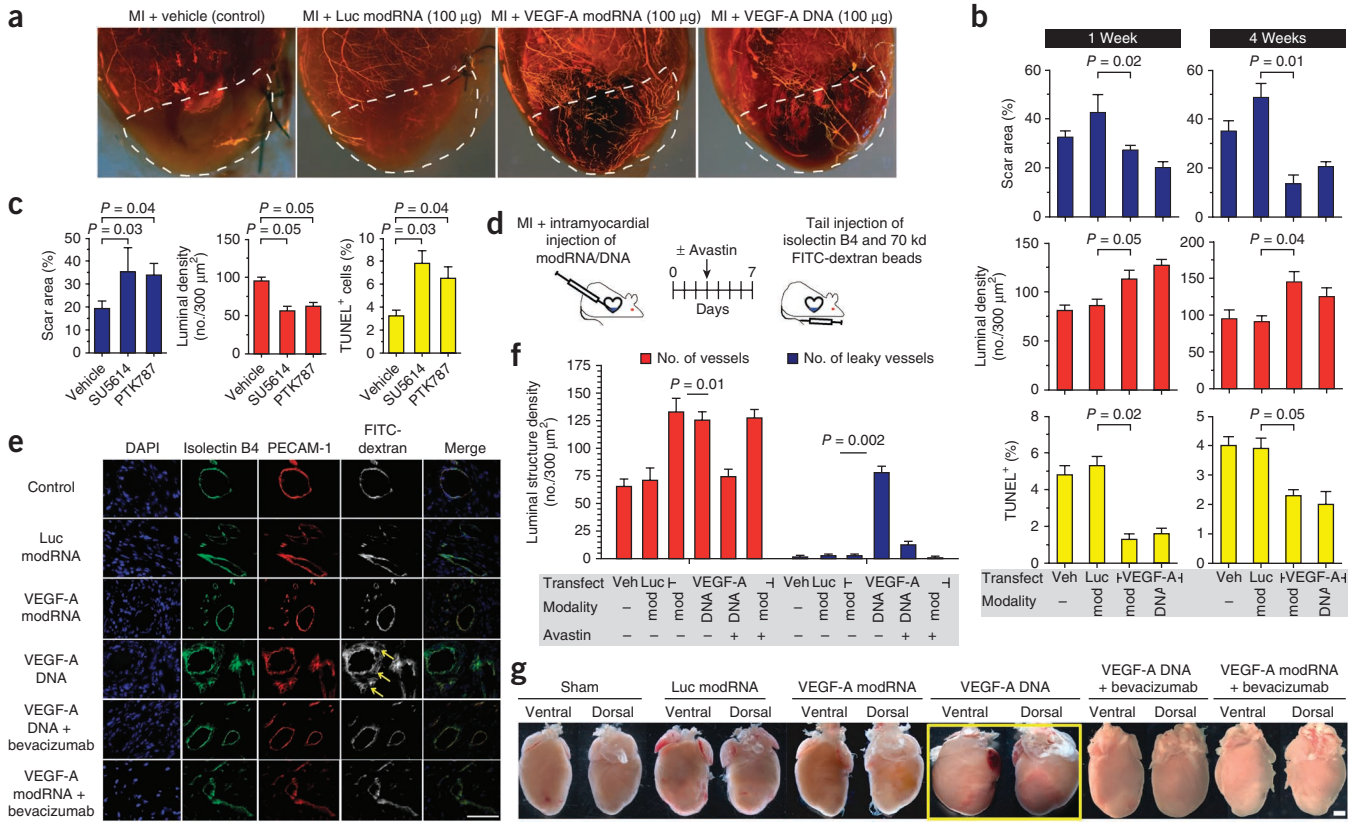

Figure 2 VEGF-A modRNA enhanced formation of functional, nonleaky vessels. (**a**) VEGF-A modRNA, injected into the infarct region at the time of experimental myocardial infarction (MI), increased vascular density in the peri-infarct region. Seven days after myocardial infarction, the vascular plexus was highlighted by Microfil followed by imaging of cleared hearts. The indicated treatments were injected within the region demarcated by the dashed lines. (**b**) VEGF-A modRNA reduced scar area and TUNEL⁺ cells and increased capillary density at 1 week and 4 weeks after myocardial infarction. Capillary density and TUNEL⁺ fraction were measured in infarct border zone (left ventricle). Masson's trichrome was used to evaluate scar area (**Supplementary Fig. 4**). $n = 3$. Error bars, s.d. (**c**) Beneficial activity of VEGF-A modRNA required KDR signaling. Mice were treated with myocardial infarction and VEGF-A modRNA. KDR inhibitors SU5614 or PTK787, administered from one day before myocardial infarction to tissue collection at 7 d after myocardial infarction, blocked beneficial effect of VEGF-A modRNA. (**d**) Experimental design to assess functional angiogenesis. VEGF-A modRNA was injected into the myocardium at the time of LAD ligation. After 1 week, isolectin B4 and FITC-dextran beads (70 kDa) were injected into the tail vein to assess connection to the systemic vasculature and vascular permeability, respectively. (**e**) Vessels formed under the influence of VEGF-A DNA, but not VEGF-A modRNA, or VEGF-A DNA with bevacizumab, neutralizing VEGF-A antibodies (given intraperitoneally twice a week) were permeable to FITC-dextran (yellow arrows). Scale bar, 50 µm. (**f**) Density of luminal structures and leaky vessels quantification for different treatments. (**g**) Macroscopic myocardial edema in hearts treated with VEGF-A DNA (yellow frame), but not with VEGF-A modRNA. Scale bar, 5 mm. *For **a**–**g**, $n = 3$, representative of two independent experiments.

© 2013 Nature America, Inc. All rights reserved.

baseline at 144–150 h (**Fig. 1c**). These kinetics differed considerably from luciferase DNA, which peaked at 72 h and retained a high signal for more than 10 d after injection.

To examine cardiac cell types transduced by modRNA, we injected Cre recombinase DNA plasmid or modRNA into Rosa26-lox-stop-lox-LacZ ($R26^{fsLacZ}$) mouse hearts, followed by 5-bromo-4-chloro-3-indolyl-β-D-galactoside (X-gal) staining for Cre-activated β-galactosidase (blue stain, **Fig. 1d–j**). Whereas using DNA plasmids resulted in infrequent cell transfection (**Fig. 1e–g**), the vast majority of cells in the injection region were transfected by modRNA, including endothelial cells (~90%), cardiomyocytes (~80%) and smooth muscle cells (~90%) (**Fig. 1h–j**). A single injection of modRNA into the cardiac apex efficiently transfected a substantial area of myocardium (~25% of the left ventricle), a level of transfection that was at least ten times greater than that achieved by injection of naked plasmid DNA (**Fig. 1k**). Similarly efficient *in vivo* modRNA transfection was observed in skeletal muscle (**Supplementary Fig. 2**).

VEGF-A modRNA improves myocardial outcome after myocardial infarction

The pulse-like kinetics of modRNA gene delivery led us to hypothesize that modRNA might be an effective means to deliver paracrine factors that could alter progenitor cell fate and thereby durably modify organ injury responses. We therefore set out to determine whether VEGF-A modRNA has beneficial activity in myocardial infarction, and we compared its performance to traditional, nonviral, VEGF-A delivery by plasmid DNA. First, we examined the kinetic profile of VEGF-A expression after VEGF-A modRNA administration *in vivo* and *in vitro*. Previous work established that cardiac VEGF-A ectopic expression does not elevate VEGF-A protein levels in serum[31]. In our *in vitro* experiments, however, cardiac cells transfected with VEGF-A modRNA translated and secreted VEGF-A protein with pulse-like kinetics that peaked rapidly and declined to basal levels after 2–3 d (**Fig. 1l**). In contrast, transfection with VEGF-A DNA plasmid induced a much broader secretion profile that peaked at a lower level at 3 d and gradually declined, with protein levels remaining above baseline at day 10.

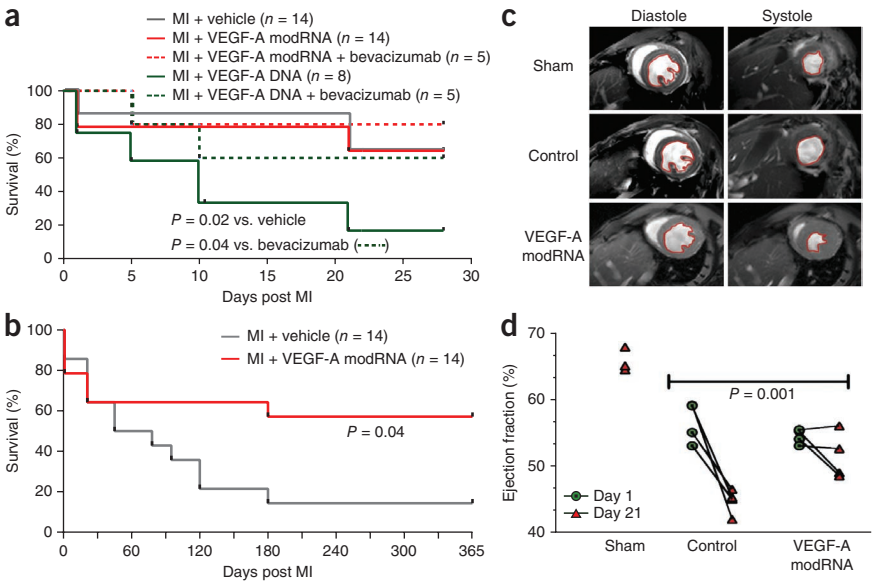

Figure 3 VEGF-A modRNA improved outcome in a mouse myocardial infarction model. (**a**) Short-term survival curve after myocardial infarction and the indicated treatments. VEGF-A modRNA, DNA or vehicle were injected into the infarct region at the time of LAD ligation. Bevacizumab was injected twice weekly starting on post-myocardial infarction day 3. *P*-values were calculated using the Mantel-Cox log-rank test. (**b**) Long-term survival curve after myocardial infarction and VEGF-A modRNA or control treatments. VEGF-A modRNA improved survival at 1 year compared to control treatment. *P*-value was calculated as in **a**. (**c**) MRI assessment of left ventricular systolic function. Images show left ventricular chamber (outlined in red) in diastole and systole. (**d**) Left ventricular systolic function (ejection fraction) was better preserved 21 d after LAD ligation in the VEGF-A modRNA group compared to control. *P*-value was calculated using paired *t*-test. Sham control, $n = 3$, control or VEGF-A modRNA group, $n = 5$.

© 2013 Nature America, Inc. All rights reserved.

Next, we evaluated the toxicity and immunogenicity of VEGF-A modRNA *in vitro* and *in vivo*. VEGF-A modRNA induced greater VEGF-A protein secretion than VEGF-A mRNA (**Supplementary Fig. 3a**). Unlike mRNA, modRNA did not cause apoptosis or upregulation of RIG-1, INF-α or INF-β, hallmarks of the innate immune response (**Supplementary Fig. 3b–c**). VEGF-A modRNA likewise exhibited minimal immunogenicity when delivered to skeletal muscle *in vivo* (**Supplementary Fig. 3c**). In addition, DNA plasmid delivery *in vivo* into cardiac muscle upregulated INF-β and RIG-1. These results are consistent with prior studies that demonstrated low modRNA toxicity and immunogenicity[1–5,32] and immunogenicity of DNA plasmid[33,34]. Together, these data show that modRNA is an efficient and nontoxic approach for transient, highly efficient and localized gene delivery to heart and skeletal muscle.

To assess the efficacy of VEGF-A modRNA in the mouse myocardial infarction model, we administered it at the time of coronary artery ligation by direct intramyocardial injection into the ischemic region. VEGF-A modRNA stimulated formation of systemically perfused vessels in the area of injection (**Fig. 2a**). Both VEGF-A modRNA and VEGF-A DNA reduced infarct size and apoptotic cell frequency, and increased capillary density at 1 and 4 weeks after myocardial infarction (**Fig. 2b**, $P \leq 0.05$; **Supplementary Fig. 4**). These beneficial effects required VEGF-A signaling through its canonical receptor KDR (also known as VEGFR2), because they were blocked by either SU5614 or PTK787, specific small-molecule inhibitors of KDR (**Fig. 2c**; $P \leq 0.05$).

Although both VEGF-A modRNA and DNA increased myocardial capillary density and reduced infarct size and cell death, the vessels formed by these treatments were functionally different. In VEGF-A DNA–treated hearts, vessels showed excessive permeability as demonstrated by extravasation of 70-kd dextran beads (**Fig. 2d–f**). In contrast, vessels in VEGF-A modRNA–treated hearts did not show this abnormal vascular permeability (**Fig. 2d–f**). The difference in vascular permeability was readily apparent on inspection of hearts: VEGF-A modRNA–treated hearts were similar in shape to control hearts, whereas VEGF-A DNA–treated hearts displayed obvious edema (**Fig. 2g**). This difference in vessel function was likely due to prolonged exposure to VEGF-A with DNA-mediated gene transfer, as increased vascular permeability is a known consequence of lengthy VEGF-A expression[35–37]. To further evaluate the importance of expression kinetics on outcome, we administered bevacizumab (Avastin), a neutralizing antibody specific for transfected human VEGF-A starting at 3 d after myocardial infarction. Bevacizumab did not detectably affect VEGF-A modRNA activity in increasing vessel density (**Fig. 2d–g**) but it blocked vessel induction by VEGF-A DNA, consistent with the differing expression kinetics of each modality. On the other hand, bevacizumab reduced the abnormal vascular permeability and edema induced by VEGF-A DNA. These data indicate that the rapid, brief pulse of VEGF-A delivered by modRNA stimulated growth of functional vessels, whereas the more prolonged VEGF-A expression delivered by DNA stimulated formation of leaky vessels.

We next evaluated the effect of VEGF-A modRNA and DNA on short-term survival after myocardial infarction (**Fig. 3a**). Although VEGF-A DNA augmented vessel number, it caused increased mortality compared to vehicle controls ($P = 0.02$ versus vehicle control), consistent with earlier reports[28]. This detrimental effect was likely due to increased vascular permeability and cardiac edema from prolonged VEGF-A exposure, because bevacizumab blockade of human VEGF-A beginning on post-myocardial infarction day 3 restored mortality to control levels ($P = 0.04$ in presence versus absence of bevacizumab). Unlike VEGF-A DNA, VEGF-A modRNA did not have an adverse effect on short-term survival, and, consistent with VEGF-A modRNA expression kinetics, this was not significantly changed by bevacizumab given 3 d after myocardial infarction (**Fig. 3a**). Together, these data point to the importance of VEGF-A expression kinetics mediated by different gene expression systems in determining their biological effect (**Supplementary Table 3**).

To assess the long-term effect of VEGF-A modRNA on outcome after myocardial infarction, we monitored the survival of control mice and mice treated with VEGF-A modRNA for a year after myocardial infarction. VEGF-A DNA–treated mice were not included in this long-term study because of their poor survival in the first month following MI. In the control group, the 1-month survival was ~60%, similar to that in other reported studies[38–40]. Survival was significantly higher in the VEGF-A modRNA group than in controls at this late end point (**Fig. 3b**; $P = 0.04$; $n = 14$). The beneficial effect of VEGF-A modRNA on survival was reflected in its effect on cardiac function, as determined by cardiac magnetic resonance imaging (MRI) measurement of cardiac ejection fraction (EF; **Fig. 3c,d**). At day 1 following myocardial infarction, EF was reduced to a similar extent in

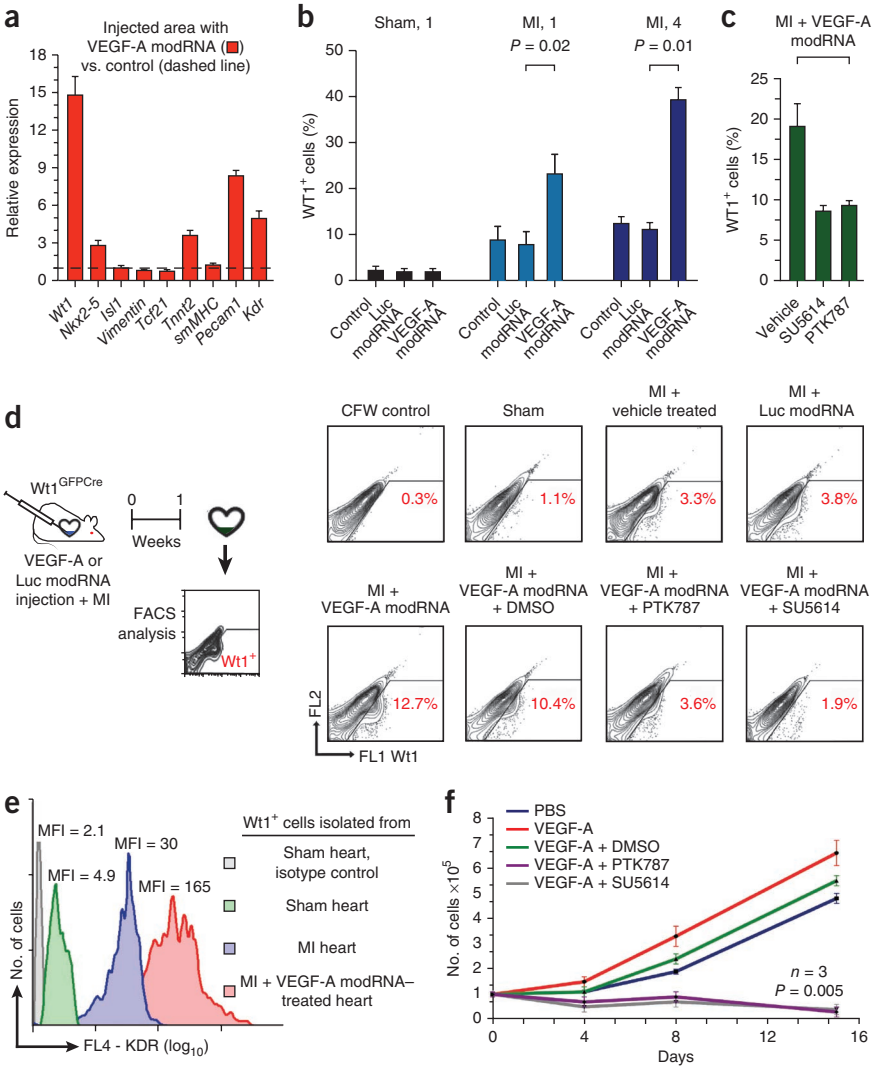

Figure 4 VEGF-A modRNA reduced scar area and apoptosis and increased capillary density and WT1+ cells proliferation after myocardial infarction in a KDR-dependent manner. (**a**) Marker gene analysis showed that VEGF-A modRNA dramatically upregulated *Wt1* expression. qRT-PCR was performed on peri-infarct tissue 3 d after myocardial infarction. Expression was calculated relative to vehicle-treated heart (dashed line). (**b**) Quantification of Wt1+ cells in the infarct border zone (left ventricle) of immunostained heart sections. VEGF-A modRNA increased frequency of WT1+ cells at 1 week and 4 weeks after myocardial infarction but not after sham treatment. (**c**) Increase in Wt1+ cells in myocardial infarction + VEGF-A modRNA–treated hearts required signaling through KDR. Samples were analyzed as in **b**, 1 week after myocardial infarction. (**d**) FACS-based quantitation of Wt1+ cells after myocardial infarction and control or VEGF-A modRNA treatment. WT1+ epicardial progenitors were isolated from dissociated $Wt1^{GFPCre}$ heart by GFP FACS sorting. VEGF-A modRNA treatment increased the frequency of GFP+ (Wt1-expressing) cells 1 week after myocardial infarction. Red numbers within the region of interest indicate the fraction of cells that were GFP+ (WT1+). (**e**) KDR expression on WT1+ epicardial progenitors was measured by FACS. Dissociated $Wt1^{GFPCre/+}$ hearts were stained for KDR, then analyzed by FACS. The histogram shows KDR immunostaining intensity on WT1+ epicardial progenitors (GFP+). Myocardial infarction and VEGF-A modRNA treatment increased KDR mean fluorescence intensity (MFI) on these progenitors. (**f**) VEGF-A protein increased, and KDR antagonists reduced proliferation of FACS-purified WT1+ epicardial progenitors. Cell number was measured using an automated cell counter at days 4, 8 and 14 of cell culture. *For **a**–**f**, $n = 3$, representative of two independent experiments. Error bars, s.d.

© 2013 Nature America, Inc. All rights reserved.

control and VEGF-A modRNA groups, indicating equivalent severity of myocardial injury (**Fig. 3d**). At 21 d after myocardial infarction, EF was better preserved in the VEGF-A modRNA group (**Fig. 3d**; $P = 0.001$, $n = 4$; **Supplementary Movies 1–3**). Consistent with declining heart function in controls compared to VEGF-A modRNA treatment, heart rate increased between days 1 and 21 after myocardial infarction in controls, and this effect was blocked by VEGF-A modRNA (**Supplementary Fig. 5**). Other MRI indices were not significantly different between groups (**Supplementary Fig. 5**). MRI assessment at later time points was not done because excess mortality in the control group would have introduced strong survivor bias. Collectively these data indicate that VEGF-A modRNA has sustained beneficial effects on myocardial outcome and on long-term survival after myocardial infarction.

VEGF-A modRNA activates epicardial cardiac progenitor cells through KDR

To further investigate mechanisms that underlie the beneficial activity of VEGF-A modRNA, we measured the expression of known cardiovascular progenitor and differentiated cell lineage markers in peri-infarct tissue of control and VEGF-A modRNA–treated hearts. qRT-PCR analysis showed upregulation of the cardiomyocyte marker *Tnnt2* and the endothelial cell markers *Pecam1* and *Kdr* (**Fig. 4a** and **Supplementary Fig. 6**). Among cardiac progenitor markers, Wilms' tumor gene 1 (*Wt1*) was highly upregulated by VEGF-A modRNA compared to control treatment, whereas other heart progenitor markers, such as *Isl1* (refs. 7–11) and *Nkx2-5*, were not substantially changed (**Fig. 4a** and **Supplementary Fig. 6**). In the heart, *Wt1* is a marker of an epicardial progenitor population that has an important role in heart injury responses[16]. Upregulation of *Wt1* was confined to the heart and was not observed in other compartments including those that might be sources of blood-borne cells (**Supplementary Fig. 7**). *Wt1* upregulation by VEGF-A modRNA suggested that the VEGF-A pulse affected the epicardial progenitor population. We confirmed a marked increase in WT1+ cells in the peri-infarct region by immunohistochemistry (**Fig. 4b**). Notably, this amplification of WT1+ cells by VEGF-A modRNA required activation of epicardial cells by injury, as it was not observed in VEGF-A modRNA–treated, sham-operated hearts (**Fig. 4b**). KDR inhibition by either SU5614 or PTK787 blocked the effect of VEGF-A modRNA (**Fig. 4c**), indicating that KDR action requires canonical VEGF-A signaling through the KDR receptor. These results were confirmed in an unbiased and independent fluorescence-activated cell sorting (FACS)-based approach that took advantage of the $Wt1^{GFPCre}$ mouse line, in which a GFP-Cre fusion protein is knocked into the endogenous *Wt1* locus[15]. Consistent with quantification of WT1+ cells by immunohistochemistry, FACS-based quantification of

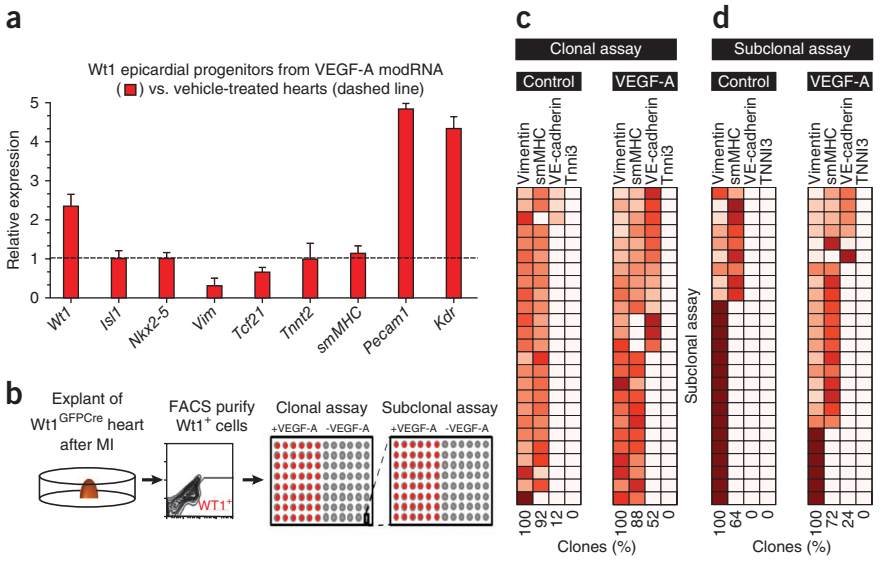

Figure 5 VEGF-A modRNA induced WT1+ epicardial progenitor proliferation and shifted differentiation toward the endothelial lineage. (**a**) VEGF-A modRNA increased endothelial marker gene expression in FACS-purified GFP+ cells after myocardial infarction. Gene expression, determined by qRT-PCR, was calculated relative to GFP+ cells isolated from control-treated, post-myocardial infarction hearts. $n = 3$, representative of two independent experiments. (**b**) Experimental design of clonal assays to assess VEGF-A modulation of WT1+ epicardial cell fate decisions. Individual FACS-purified cardiac WT1+ cells were deposited in 96-well dishes, clonally expanded and assessed for differentiation to the indicated lineages by qRT-PCR. One VEGF-A–naive, VE-cadherin–negative clone was subcloned and the individual subclones were further tested in the clonal differentiation assay. (**c**) VEGF-A modRNA promoted Wt1+ epicardial progenitor differentiation toward the endothelial lineage. Each row represents an individual clone, and each column indicates the relative qRT-PCR–measured expression of the indicated lineage marker. The percentage of clones with detectable expression of each lineage marker is indicated at the bottom of each column. (**d**) VEGF-A modRNA effect on Wt1+ epicardial progenitor differentiation was recapitulated in the subclonal assay. This confirmed multipotency of WT1+ epicardial cells and made polyclonal contamination highly unlikely.

© 2013 Nature America, Inc. All rights reserved.

the number of WT1+ cells by GFP signal showed that myocardial infarction alone substantially expanded this cell population (**Fig. 4d**), as we reported previously[16]. VEGF-A modRNA, but not Luc modRNA, further strongly amplified this population by about fourfold. Again, this effect was blocked by KDR inhibitors SU5614 and PTK787.

To determine whether VEGF-A acts directly on WT1+ epicardial progenitors to drive their amplification, we measured the abundance of KDR receptors on these cells by FACS (**Fig. 4e**). In sham-operated hearts, WT1+ cells expressed low levels of the KDR receptor (mean KDR fluorescence intensity was about twofold above isotype control background). WT1+ cell expression of the KDR receptor increased dramatically (about sixfold) after myocardial infarction, and VEGF-A modRNA treatment further upregulated KDR expression by 5.5-fold, indicating a positive-feedback response in which VEGF-A reinforces KDR expression, as previously noted in endothelial cells[41]. Upregulation of KDR after myocardial infarction coincides with the general activation of numerous epicardial genes after injury[16] and likely accounts for the requirement of myocardial infarction to enable WT1+ epicardial cells to respond to VEGF-A modRNA (**Fig. 4b**). To further determine whether VEGF-A acts directly on post-myocardial infarction WT1+ epicardial cells, we purified these cells by FACS and measured their proliferation in response to recombinant VEGF-A (**Fig. 4f**). VEGF-A increased proliferation of cultured WT1+ epicardial cells, and KDR inhibition powerfully blocked their proliferation. These data indicate that VEGF-A acts directly through KDR on activated, post-myocardial infarction WT1+ epicardial progenitors.

VEGF-A modRNA induced WT1+ epicardial progenitor differentiation into endothelial cells *in vitro*

During heart development, WT1+ epicardial progenitors undergo an epithelial-to-mesenchymal transition. The resulting epicardium-derived cells (EPDCs) migrate into the myocardium and predominantly differentiate into fibroblasts and smooth muscle cells. Infrequently, EPDCs contribute to the endothelial lineage[15,42], and they have also been found to differentiate into cardiomyocytes[13,17,42]. VEGF-A modRNA increased capillary density and upregulated endothelial markers in peri-infarct tissue (**Fig. 2b**). We hypothesized that VEGF-A might alter the fate of the WT1+ epicardial progenitors and enhance their endothelial differentiation. qRT-PCR analysis of FACS-purified, post-myocardial infarction, WT1+ epicardial progenitors indicated that VEGF-A modRNA strongly upregulated expression of endothelial markers *Pecam1* and *Kdr* (**Fig. 5a**). VEGF-A stimulation of endothelial differentiation of epicardial progenitors was further demonstrated by culturing FACS-purified, post-myocardial infarction, Wt1+ cells for 7 d in the presence or absence of recombinant VEGF-A. Analysis of marker genes by qRT-PCR revealed that VEGF-A stimulation strongly upregulated endothelial markers *VE-Cadherin*, *Pecam1* and *Kdr* (**Supplementary Fig. 8a**). This result was corroborated by FACS analysis, which showed that VEGF-A treatment markedly increased the frequency of KDR+/VE-cadherin+ endothelial cells (68% versus 14%; **Supplementary Fig. 8b**), and by immunofluorescence imaging, which demonstrated co-expression of VE-cadherin and GFP (expressed from Wt1GFPCre) in cultures stimulated by VEGF-A (**Supplementary Fig. 8c**).

We further tested the hypothesis that VEGF-A influences WT1+ epicardial progenitor cell lineage decisions using an *in vitro* clonal assay. FACS-purified, post-myocardial infarction, WT1+ epicardial cells were individually plated in 96-well dishes, clonally expanded and assessed for differentiation into the major cardiac lineages in the presence or absence of recombinant VEGF-A by qRT-PCR (**Fig. 5b**). This assay demonstrated the multipotency of WT1+ epicardial progenitors at the clonal level (**Fig. 5c**). VEGF-A treatment for 7 d increased the fraction of clones that were positive for the endothelial marker *VE-Cadherin* from 12% to 52% (**Fig. 5c**). To further demonstrate that this was a clonal event rather than polyclonal contamination of endothelial cells, we subcloned a clone that was initially *VE-Cadherin* negative in the absence of VEGF-A and repeated the clonal differentiation assay. VEGF-A again strongly stimulated differentiation toward an endothelial fate (24% versus 0%, **Fig. 5d**). These clonal assays confirm the multipotency of WT1+ epicardial progenitor cells, and demonstrate at the clonal level that VEGF-A biases epicardial progenitor fate decisions toward the endothelial lineage.

In summary, these studies identify epicardial progenitors as a target for VEGF acting as a vasculogenic cell fate switch, in addition to its

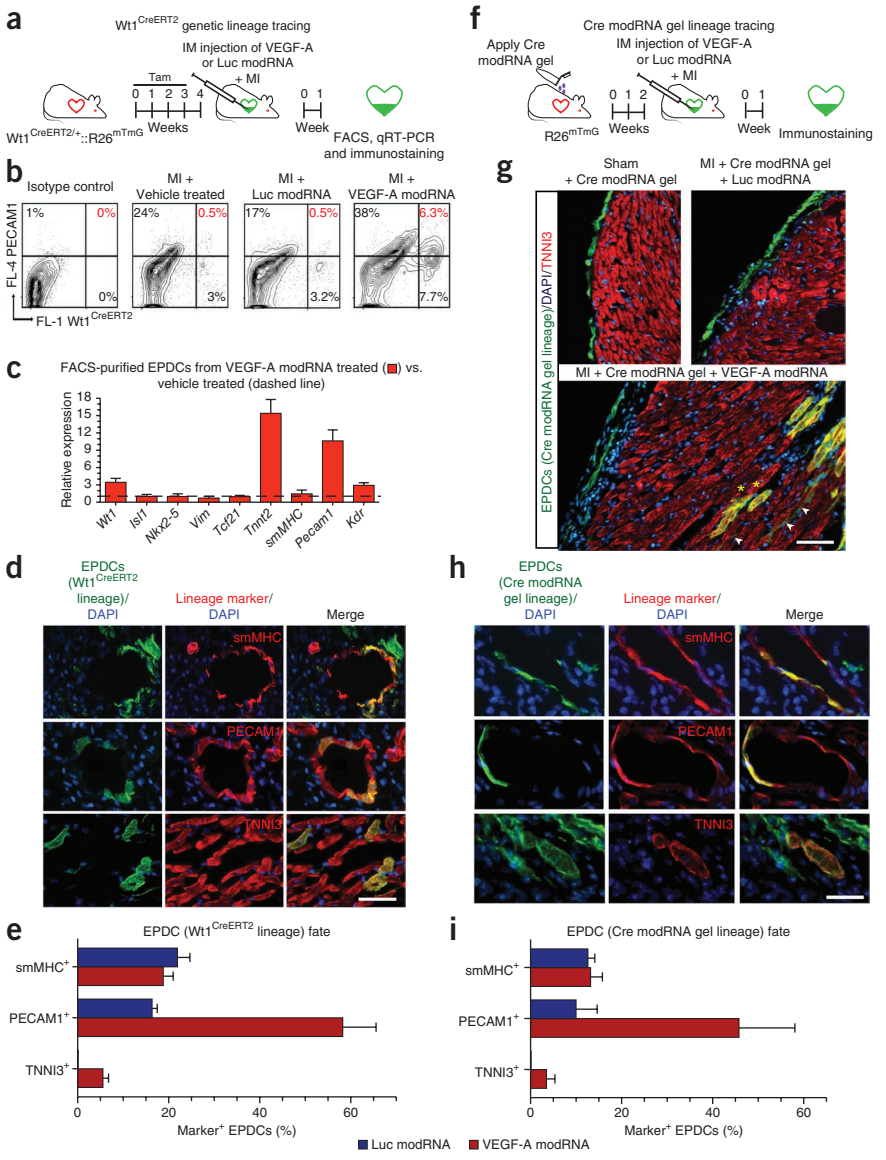

Figure 6 VEGF-A modRNA promoted differentiation of EPDCs toward the cardiovascular lineage *in vivo*. (**a**) Genetic lineage tracing was used to follow the fate of EPDCs after myocardial infarction with VEGF-A or Luc modRNA treatment. Tamoxifen treatment of $Wt1^{CreERT2/+}$::$R26^{mTmG}$ mice before myocardial infarction irreversibly labeled epicardial cells and their descendants with GFP. (**b**) FACS analysis of dissociated hearts 1 week after myocardial infarction indicated that VEGF-A modRNA increased the frequency of EPDCs expressing the endothelial marker PECAM1 (% indicated in red). (**c**) VEGF-A modRNA increased endothelial and cardiomyocyte marker gene expression in FACS-sorted EPDCs 1 week after myocardial infarction. Expression of each marker was measured by qRT-PCR and displayed relative to expression in control-treated EPDCs. (**d**) Immunofluorescent analysis of EPDC fate by $Wt1^{CreERT2}$ genetic lineage tracing. Expression of smooth muscle (smMHC), endothelial (PECAM1) and cardiomyocyte (TNNI3) markers by GFP^+ EPDCs was assessed by immunostaining and confocal microscopy. Scale bar, 30 μm. (**e**) Quantification of **d**. A minimum of 2,000 EPDCs were analyzed in each post-myocardial infarction heart treated with Luc modRNA ($n = 2$) or VEGF-A modRNA ($n = 5$) from two independent experiments. The graph shows the percentage of GFP^+ EPDCs that co-expressed the indicated lineage marker. (**f**) Cre modRNA gel-mediated tracing of epicardial cell fate was used to follow the fate of EPDCs after myocardial infarction with VEGF-A or Luc modRNA treatment. Cre modRNA gel, applied to $R26^{mTmG}$ mice 2 weeks before myocardial infarction, irreversibly labeled epicardial cells and their descendants with GFP. (**g**) Cre modRNA gel selectively labeled epicardial cells with GFP in $R26^{mTmG}$ mice. Note that labeled cells were restricted to the epicardium in controls (sham or myocardial infarction and Luc modRNA treatment). However in myocardial infarction hearts injected with VEGF-A modRNA, labeled cells were found both in the epicardial layer and within the myocardium and differentiated into myocytes (yellow asterisks) and nonmyocytes (white arrowheads). Scale bar, 50 μm. (**h**) Immunofluorescent analysis of EPDC fate with Cre modRNA gel lineage tracing. Scale bar, 30 μm. (**i**) Quantification of **h**. A minimum of 2,000 Cre-gel–labeled cells were analyzed in each post-myocardial infarction heart treated with Luc modRNA ($n = 3$) or VEGF-A modRNA ($n = 4$) from two independent experiments. Error bars, s.d. The graph shows the percentage of GFP^+ EPDCs that co-expressed the indicated lineage marker.

© 2013 Nature America, Inc. All rights reserved.

already well-known effect on promoting the proliferation of already differentiated endothelial cells.

VEGF-A modRNA induced WT1+ epicardial cell differentiation into endovascular cell types *in vivo*

To directly track the fate of EPDCs to different lineages after myocardial infarction, we performed genetic lineage tracing using $WT1^{CreERT2/+}$ mice, in which tamoxifen-activated CreERT2 was expressed from the endogenous *Wt1* locus[16]. Treatment of adult mice with tamoxifen triggered recombination of the $R26^{mTmG}$ reporter[43] in *Wt1*-expressing cells, irreversibly labeling them with membrane-localized GFP and simultaneously inactivating expression of membrane-localized tomato fluorescent protein. We defined these cardiac GFP^+ cells, consisting of *Wt1*-expressing cells and their descendants, as EPDCs[16]. After allowing clearance of tamoxifen for 1 week, myocardial infarction was induced by injection of VEGF-A or Luc (control gene) modRNA into the peri-infarct zone. After 7 d, the fate of $Wt1^{CreERT2}$-labeled EPDCs was evaluated by FACS, qRT-PCR and immunofluorescent imaging (**Fig. 6a–e** and **Supplementary Fig. 9**). VEGF-A modRNA increased the number of EPDCs four-fold (**Fig. 6b**). The fraction of $PECAM1^+$ cells was 26% greater in VEGF-A modRNA versus Luc modRNA hearts (44% versus 18%). Therefore, we estimate that ~23% (6% of $Wt1^{CreERT2}$-labeled EPDCs / 26% total endothelial cells) of the VEGF-A–stimulated increase in $PECAM1^+$ cells arose from EPDCs. This result was supported by qRT-PCR of FACS-purified EPDCs, which showed that VEGF-A modRNA increased expression of *Pecam1* and *Kdr* (**Fig. 6c**). Moreover, EPDCs in the VEGF-A modRNA group upregulated the cardiomyocyte marker *Tnnt2*, suggesting that VEGF-A enhanced EPDC differentiation toward the cardiomyocyte lineage.

Confocal analysis of immunostained sections further substantiated these conclusions. In controls without injury or with myocardial

infarction and vehicle treatment, EPDCs stayed on the epicardial surface of the heart[16] (**Supplementary Fig. 9**). In contrast, myocardial infarction and VEGF-A modRNA mobilized EPDCs so that they migrated into the myocardium (**Supplementary Fig. 9**) and increased differentiation toward the endothelial lineage (58% with VEGF-A modRNA versus 16% with Luc modRNA; **Fig. 6d**,**e**). We also detected EPDCs that co-expressed the cardiomyocyte marker TNNI3 in VEGF-A modRNA hearts, but not in controls (5% versus 0%, respectively; **Fig. 6d**,**e**). It is unlikely that this result was due to VEGF-A–induced upregulation of *Wt1* (and therefore the CreERT2 lineage tracer) in cardiomyocytes, as qRT-PCR indicated that VEGF-A had no effect on adult cardiomyocyte *Wt1* expression (**Supplementary Fig. 10**). Furthermore, tamoxifen labeling was done before either myocardial infarction or VEGF-A modRNA treatment, and the level of tamoxifen-independent Cre activity in myocardial infarction and VEGF-A modRNA–treated hearts was trivial (0.005% of cardiomyocytes and 0.003% of endothelial cells were GFP^+).

To confirm our results using an independent system that did not critically depend on *Wt1*-driven marker alleles, we used a Cre modRNA–containing biocompatible gel to selectively label and trace the fate of epicardium-derived cells in the adult heart (**Fig. 6f**). When applied to $R26^{mTmG}$ hearts, Cre modRNA gel selectively labeled cells in the epicardial layer (**Fig. 6g**). We tested the kinetics of gene transfer by means of modRNA gel by applying Luc modRNA gel onto the hearts of CFW strain mice (**Supplementary Fig. 11a**,**b**). Luciferase bioluminescence was detected at near-peak levels by 3 h and peak levels at 24 h, and it was no longer detectable at 72 h. Similarly, Cre modRNA gel expressed Cre protein in cells confined to the epicardial layer 2 d after gel application, but Cre protein was no longer detectable at 14 d (**Supplementary Fig. 11c**).

Based on these data, we developed a Cre modRNA gel-based prelabeling strategy (**Fig. 6f**) that minimized the possibility of nonepicardial labeling in the complex environment induced by the myocardial infarction. We applied Cre modRNA gel to the heart to label epicardial cells, waited 2 weeks for decay of Cre activity, and then performed LAD ligation and concurrent myocardial injection of VEGF-A or Luc modRNA into the infarct region. One week later, we assessed the fate of Cre modRNA–labeled EPDCs by confocal analysis of immunostained cryosections. Consistent with the $Wt1^{CreERT2}$ labeling result, EPDCs remained in the epicardial layer in control hearts with sham operations or hearts with myocardial infarction plus Luc modRNA. In contrast, myocardial infarction plus VEGF-A modRNA mobilized EPDCs from the epicardial layer and allowed their migration into the myocardium (**Fig. 6g** and **Supplementary Fig. 12**). EPDCs co-expressed smooth muscle, endothelial and cardiomyocyte lineage markers (**Fig. 6h** and **Supplementary Fig. 12**). Quantification of the percentage of EPDCs expressing each lineage marker showed that VEGF-A modRNA directed EPDCs toward an endothelial fate (48% versus 9%), and led to a small but reproducible subset of EPDCs co-expressing cardiomyocyte markers (**Fig. 6g–i**). Collectively, the $Wt1^{CreERT2}$ and Cre modRNA gel fate mapping experiments demonstrate through two independent approaches that VEGF-A modRNA alters EPDC fate in the postnatal heart, driving EPDC differentiation into endothelial cells and potentially to cardiomyocytes.

DISCUSSION

Our study advances an approach to solid-organ repair and regeneration in which delivery of appropriate signal(s) at the right time and place modifies endogenous progenitor cell activity and thereby promotes longstanding therapeutic benefits. We show that modRNA is an effective, robust approach to implement this approach. modRNA avoids several of the apparent problems that have arisen with conventional cardiac gene therapy vectors[30,44], including lack of genomic integration, persistence of expression, immunogenicity, difficulty in scalability and production, need for life-long monitoring for tumorigenesis and other adverse clinical outcomes, and the potential for vector escape into the systemic circulation and long-term expression elsewhere in the body. For these reasons, modRNA has considerable translational potential.

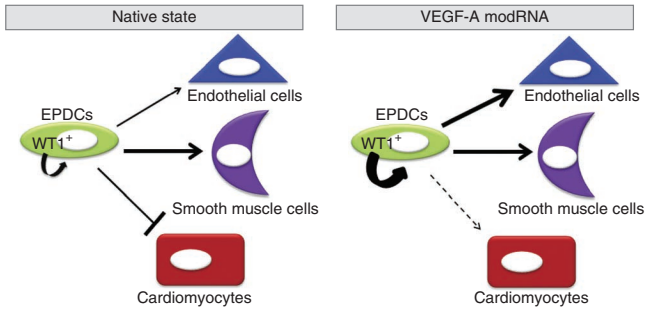

Figure 7 Suggested model for the role of VEGF-A modRNA on EPDCs differentiation *in vivo*. Schematic summary of results. In the native state, myocardial infarction stimulates amplification of $WT1^+$ EPDCs, which remain confined to the epicardial layer. VEGF-A modRNA, in the context of myocardial infarction, augments amplification of $WT1^+$ EPDCs, increases their mobilization into the myocardial layer and enhances their differentiation toward the endothelial lineage.

One of the keys to paracrine signal therapeutics is to deliver a transient, strong signal at a time and place that coincides with initial activation of an endogenous progenitor pool. As shown in this study, a transient pulse delivered in this manner can achieve long-term benefit through modification of progenitor cell activity and fate. Specifically, we demonstrated that a single intramyocardial injection of VEGF-A modRNA improved myocardial outcome and survival after myocardial infarction. This salutary response was due to improved formation of functional vessels in the peri-infarct region, which is associated with altered activity of epicardial progenitors. Pulse-like VEGF-A expression after myocardial infarction amplified the $WT1^+$ epicardial progenitor pool and enhanced their differentiation toward the endothelial lineage (**Fig. 7**), forming a substantial subset of the additional endothelial cells generated under VEGF-A stimulation. This VEGF-A effect on epicardial progenitors is reminiscent of the effect of VEGF-A on multipotent *Isl1* heart progenitors that we recently reported[29], and indeed VEGF-A may similarly affect other cardiac progenitor populations. The unique kinetics of modRNA delivery were required to obtain benefit, as it permitted pulse-like VEGF-A delivery at precisely the time that myocardial injury activates epicardial cells from their quiescent state in the normal heart. The transient nature of VEGF-A modRNA delivery was also crucial, as sustained VEGF-A delivery by DNA injection led to adverse effects on vascular function.

EDPC lineage tracing using several different genetic labels has indicated that a subset of EPDCs differentiate into cardiomyocytes under certain conditions in the developing and adult heart[6,12,13,45,46]. Consistent with prior studies[15,16], we found that adult EPDCs have little native potential to differentiate toward the cardiomyocyte lineage. However, VEGF-A stimulation appeared to increase cardiomyocyte differentiation to consistently detectable, albeit low, levels. We confirmed this result using an independent lineage tracing system, bolstering the evidence that EPDCs differentiate into cardiomyocytes. However, given the pitfalls and limitations of genetic lineage tracing approaches[47,48] and the lack of cardiomyocyte differentiation in the *in vitro* clonal assay (which might be attributable to inadequacies of

© 2013 Nature America, Inc. All rights reserved.

the *in vitro* culture system), additional studies are needed to further support this conclusion. The number of cardiomyocytes formed by EPDCs was reproducible but low and likely not sufficient to account for the therapeutic benefit of VEGF-A modRNA. Nevertheless, this finding suggests that additional paracrine signals might be identified that will achieve differentiation of EPDCs to cardiomyocytes at therapeutically meaningful levels.

METHODS

Methods and any associated references are available in the online version of the paper.

Note: Any Supplementary Information and Source Data files are available in the online version of the paper.

ACKNOWLEDGMENTS

This work was funded by US National Institutes of Health U01H100408 (K.R.C.), U01HL098166 (K.R.C.), U01JL100401 (W.T.P.), R01HL094683 (W.T.P.), RC1HL099618 (K.R.C., W.T.P.) and UO1HL100402 (A.J.W.). K.O.L. held a Croucher Foundation Fellowship and A.J.W. is an Early Career Scientist of the Howard Hughes Medical Institute. We thank R. Liao, J. Guan, J. Truelove, L. Bu, M. Stachel, K. Buac, V. Priestly, R. Gazit, K. Ketman, N. Barteneva, A. He, S. Stevens, B. Zhou and L.Warren for all their help in this project. Adult cardiomyocytes were a kind gift from R. Liao (Biological and Biomaterial Science, Department of Medicine, Brigham and Women's Hospital, Harvard Medical School).

AUTHOR CONTRIBUTIONS

L.Z. (lzangi@enders.tch.harvard.edu) worked in the Rossi, Chien and Pu laboratories, and designed and carried out most of the experiments, analyzed most of the data, and wrote the manuscript. K.O.L. in the Chien lab designed and performed experiments and analyzed the qRT-PCR and immunostaining data, and wrote the manuscript. Her contribution is similar in significance to the contributions of L.Z. A.v.G. performed and analyzed the *Wt1*-related experiments. Q.M. and R.G. carried out myocardial infarction experiments. W.E. carried out plasmid preparation. L.M.P. performed blinded analysis of imaging data and wrote the manuscript. D.S. performed and analyzed skeletal muscle *in vivo* transfection. H.X. performed isolation of neonatal mouse cardiomyocytes. M.T. performed and analyzed *in vitro* transfection of mouse adult myotubes. B.S. carried out and analyzed the MRI experiment. M.N., D.M.B., R.A.L. and A.J.W. designed experiments, analyzed data, and revised the manuscript. D.J.R. (Derrick.Rossi@childrens.harvard.edu) designed *in vitro* cardiomyocyte experiments and revised the manuscript. K.R.C. (kchien@harvard.edu; kenneth.chien@ki.se) conceived the initial project and experimental studies, and with W.T.P. (wpu@enders.tch.harvard.edu) designed further experiments, analyzed data, and wrote the manuscript. The initial discovery of VEGF-A as a cell fate switch for heart progenitors in general, and its effects in myocardial infarction on the expansion of epicardial heart progenitors along with vascular regeneration was made in the Chien lab (L.Z., K.O.L. and K.R.C.). The Chien lab (L.Z., K.R.C.) and the Pu lab (A.v.G., W.T.P.) worked together to extend and expand these initial results. Address correspondence on ModRNA reagents, delivery and protocols to K.R.C. and on mouse models to W.T.P.

COMPETING FINANCIAL INTERESTS

The authors declare competing financial interests: details are available in the online version of the paper.

Reprints and permissions information is available online at http://www.nature.com/reprints/index.html.

1. Kariko, K., Buckstein, M., Ni, H. & Weissman, D. Suppression of RNA recognition by Toll-like receptors: the impact of nucleoside modification and the evolutionary origin of RNA. *Immunity* **23**, 165–175 (2005).
2. Kariko, K., Muramatsu, H., Keller, J.M. & Weissman, D. Increased erythropoiesis in mice injected with submicrogram quantities of pseudouridine-containing mRNA encoding erythropoietin. *Mol. Ther.* **20**, 948–953 (2012).
3. Kariko, K. *et al.* Incorporation of pseudouridine into mRNA yields superior nonimmunogenic vector with increased translational capacity and biological stability. *Mol. Ther.* **16**, 1833–1840 (2008).
4. Kormann, M.S. *et al.* Expression of therapeutic proteins after delivery of chemically modified mRNA in mice. *Nat. Biotechnol.* **29**, 154–157 (2011).
5. Mays, L.E. *et al.* Modified Foxp3 mRNA protects against asthma through an IL-10-dependent mechanism. *J. Clin. Invest.* **123**, 1216–1228 (2013).
6. Wessels, A. *et al.* Epicardially derived fibroblasts preferentially contribute to the parietal leaflets of the atrioventricular valves in the murine heart. *Dev. Biol.* **366**, 111–124 (2012).
7. Moretti, A. *et al.* Multipotent embryonic isl1+ progenitor cells lead to cardiac, smooth muscle, and endothelial cell diversification. *Cell* **127**, 1151–1165 (2006).
8. Qyang, Y. *et al.* The renewal and differentiation of Isl1+ cardiovascular progenitors are controlled by a Wnt/beta-catenin pathway. *Cell Stem Cell* **1**, 165–179 (2007).
9. Bu, L. *et al.* Human ISL1 heart progenitors generate diverse multipotent cardiovascular cell lineages. *Nature* **460**, 113–117 (2009).
10. Laugwitz, K.L. *et al.* Postnatal isl1+ cardioblasts enter fully differentiated cardiomyocyte lineages. *Nature* **433**, 647–653 (2005).
11. Domian, I.J. *et al.* Generation of functional ventricular heart muscle from mouse ventricular progenitor cells. *Science* **326**, 426–429 (2009).
12. Chong, J.J. *et al.* Adult cardiac-resident MSC-like stem cells with a proepicardial origin. *Cell Stem Cell* **9**, 527–540 (2011).
13. Cai, C.L. *et al.* A myocardial lineage derives from Tbx18 epicardial cells. *Nature* **454**, 104–108 (2008).
14. Loffredo, F.S., Steinhauser, M.L., Gannon, J. & Lee, R.T. Bone marrow-derived cell therapy stimulates endogenous cardiomyocyte progenitors and promotes cardiac repair. *Cell Stem Cell* **8**, 389–398 (2011).
15. Zhou, B. *et al.* Epicardial progenitors contribute to the cardiomyocyte lineage in the developing heart. *Nature* **454**, 109–113 (2008).
16. Zhou, B. *et al.* Adult mouse epicardium modulates myocardial injury by secreting paracrine factors. *J. Clin. Invest.* **121**, 1894–1904 (2011).
17. Smart, N. *et al.* De novo cardiomyocytes from within the activated adult heart after injury. *Nature* **474**, 640–644 (2011).
18. Garbern, J.C. & Lee, R.T. Cardiac stem cell therapy and the promise of heart regeneration. *Cell Stem Cell* **12**, 689–698 (2013).
19. Malliaras, K. *et al.* Cardiomyocyte proliferation and progenitor cell recruitment underlie therapeutic regeneration after myocardial infarction in the adult mouse heart. *EMBO Mol. Med.* **5**, 191–209 (2013).
20. Ptaszek, L.M., Mansour, M., Ruskin, J.N. & Chien, K.R. Towards regenerative therapy for cardiac disease. *Lancet* **379**, 933–942 (2012).
21. von Gise, A. *et al.* WT1 regulates epicardial epithelial to mesenchymal transition through beta-catenin and retinoic acid signaling pathways. *Dev. Biol.* **356**, 421–431 (2011).
22. Svensson, E.C. *et al.* Efficient and stable transduction of cardiomyocytes after intramyocardial injection or intracoronary perfusion with recombinant adeno-associated virus vectors. *Circulation* **99**, 201–205 (1999).
23. Patterson, C. & Runge, M.S. Therapeutic myocardial angiogenesis via vascular endothelial growth factor gene therapy: moving on down the road. *Circulation* **102**, 940–942 (2000).
24. Hao, X. *et al.* Myocardial angiogenesis after plasmid or adenoviral VEGF-A(165) gene transfer in rat myocardial infarction model. *Cardiovasc. Res.* **73**, 481–487 (2007).
25. Eppler, S.M. *et al.* A target-mediated model to describe the pharmacokinetics and hemodynamic effects of recombinant human vascular endothelial growth factor in humans. *Clin. Pharmacol. Ther.* **72**, 20–32 (2002).
26. Dor, Y. *et al.* Conditional switching of VEGF provides new insights into adult neovascularization and pro-angiogenic therapy. *EMBO J.* **21**, 1939–1947 (2002).
27. Tafuro, S. *et al.* Inducible adeno-associated virus vectors promote functional angiogenesis in adult organisms via regulated vascular endothelial growth factor expression. *Cardiovasc. Res.* **83**, 663–671 (2009).
28. Lee, R.J. *et al.* VEGF gene delivery to myocardium: deleterious effects of unregulated expression. *Circulation* **102**, 898–901 (2000).
29. Lui, K. *et al.* Driving vascular endothelial cell fate of human multipotent Isl1+ heart progenitors with VEGF modified mRNA. *Cell Res.* doi:10.1038/cr.2013.112 (10 September 2013).
30. Djurovic, S., Iversen, N., Jeansson, S., Hoover, F. & Christensen, G. Comparison of nonviral transfection and adeno-associated viral transduction on cardiomyocytes. *Mol. Biotechnol.* **28**, 21–32 (2004).
31. Grunewald, M. *et al.* VEGF-induced adult neovascularization: recruitment, retention, and role of accessory cells. *Cell* **124**, 175–189 (2006).
32. Warren, L. *et al.* Highly efficient reprogramming to pluripotency and directed differentiation of human cells with synthetic modified mRNA. *Cell Stem Cell* **7**, 618–630 (2010).
33. Choi, M.K. *et al.* A selective contribution of the RIG-I-like receptor pathway to type I interferon responses activated by cytosolic DNA. *Proc. Natl. Acad. Sci. USA* **106**, 17870–17875 (2009).
34. Stetson, D.B. & Medzhitov, R. Recognition of cytosolic DNA activates an IRF3-dependent innate immune response. *Immunity* **24**, 93–103 (2006).
35. Su, H. *et al.* Additive effect of AAV-mediated angiopoietin-1 and VEGF expression on the therapy of infarcted heart. *Int. J. Cardiol.* **133**, 191–197 (2009).
36. Spilsbury, K., Garrett, K.L., Shen, W.Y., Constable, I.J. & Rakoczy, P.E. Overexpression of vascular endothelial growth factor (VEGF) in the retinal pigment epithelium leads to the development of choroidal neovascularization. *Am. J. Pathol.* **157**, 135–144 (2000).
37. Nagy, J.A. *et al.* Permeability properties of tumor surrogate blood vessels induced by VEGF-A. *Lab. Invest.* **86**, 767–780 (2006).
38. Noyan-Ashraf, M.H. *et al.* GLP-1R agonist liraglutide activates cytoprotective pathways and improves outcomes after experimental myocardial infarction in mice. *Diabetes* **58**, 975–983 (2009).

© 2013 Nature America, Inc. All rights reserved.

39. Sauve, M. *et al.* Genetic deletion or pharmacological inhibition of dipeptidyl peptidase-4 improves cardiovascular outcomes after myocardial infarction in mice. *Diabetes* **59**, 1063–1073 (2010).
40. Yuan, M.J. *et al.* Myocardial angiogenesis after chronic ghrelin treatment in a rat myocardial infarction model. *Regul. Pept.* **179**, 39–42 (2012).
41. Shen, B.Q. *et al.* Homologous up-regulation of KDR/Flk-1 receptor expression by vascular endothelial growth factor *in vitro*. *J. Biol. Chem.* **273**, 29979–29985 (1998).
42. Wilm, B., Ipenberg, A., Hastie, N.D., Burch, J.B. & Bader, D.M. The serosal mesothelium is a major source of smooth muscle cells of the gut vasculature. *Development* **132**, 5317–5328 (2005).
43. Muzumdar, M.D., Tasic, B., Miyamichi, K., Li, L. & Luo, L. A global double-fluorescent Cre reporter mouse. *Genesis* **45**, 593–605 (2007).
44. Hoshijima, M. *et al.* Chronic suppression of heart-failure progression by a pseudophosphorylated mutant of phospholamban via *in vivo* cardiac rAAV gene delivery. *Nat. Med.* **8**, 864–871 (2002).
45. Kruithof, B.P. *et al.* BMP and FGF regulate the differentiation of multipotential pericardial mesoderm into the myocardial or epicardial lineage. *Dev. Biol.* **295**, 507–522 (2006).
46. Katz, T.C. *et al.* Distinct compartments of the proepicardial organ give rise to coronary vascular endothelial cells. *Dev. Cell* **22**, 639–650 (2012).
47. Zhou, B. & Pu, W.T. Genetic Cre-loxP assessment of epicardial cell fate using Wt1-driven Cre alleles. *Circ. Res.* **111**, e276–e280 (2012).
48. Christoffels, V.M. *et al.* Tbx18 and the fate of epicardial progenitors. *Nature* **458**, E8–E9, E9–10 (2009).

© 2013 Nature America, Inc. All rights reserved.

ONLINE METHODS

Construction of IVT templates and synthesis of modRNA. Production of *in vitro* transcription (IVT) template constructs and subsequent RNA synthesis have been described previously[32]. All oligonucleotide reagents were synthesized by Integrated DNA Technologies (Coralville). ORFs were amplified by PCR from plasmids encoding GFP, mCherry, firefly luciferase, Cre recombinase and human VEGF-A (165) (Addgene, see **Supplementary Table 4** for ORF sequences). PCR reactions were performed with HiFi Hotstart (KAPA Biosystems) according to the manufacturer's instructions. Splint-mediated ligations were carried out with Ampligase Thermostable DNA Ligase (Epicenter Biotechnologies). UTR ligations were conducted in the presence of 200 nM UTR oligos and 100 nM splint oligos. All intermediate PCR and ligation products were purified with QIAquick spin columns (Qiagen) before further processing. Template PCR amplicons were subcloned with the pcDNA 3.3-TOPO TA cloning kit (Invitrogen). Plasmid inserts were excised by restriction digest and recovered with SizeSelect gels (Invitrogen) before being used to template Poly A tail PCRs. RNA was synthesized with the MEGAscript T7 kit (Ambion), with 1.6 µg of purified tail PCR product to template each 40 µl reaction. A custom ribonucleoside blend was used comprising 3′-*O*-Me-m7G(5′)ppp(5′)G cap analog (New England Biolabs), ATP and guanosine triphosphate (USB), 5-methylcytidine triphosphate and pseudouridine triphosphate (TriLink Biotechnologies). Final nucleotide concentrations in the reaction mixture were 6 mM for the cap analog, 1.5 mM for guanosine triphosphate and 7.5 mM for the other nucleotides. RNA was purified with Ambion MEGAclear spin columns and then treated with Antarctic Phosphatase (New England Biolabs) for 30 min at 37 °C to remove residual 5′-phosphates. Treated RNA was repurified, quantified by Nanodrop (Thermo Scientific) and precipitated with 5 M ammonium acetate according to the manufacturer's instructions. modRNA was resuspended in 10 mM Tris HCl, 1 mM EDTA at 100 ng/µl for *in vitro* use or 20–30 µg/µl for *in vivo* use.

modRNA Transfection. modRNA and RNAiMAX (Invitrogen) transfection agent were each dissolved separately in Opti-MEM (Invitrogen), combined and then incubated for 15 min at room temperature to generate the transfection mixture. 5 or 0.5 µl of RNAiMAX reagent was used for every microgram of modRNA for *in vitro* or *in vivo* transfection. *In vitro* transfection was performed by adding the transfection mixture to cells plated in DMEM with 2% FBS and 200 ng/ml B18R (eBioscience, San Diego, CA). For *in vivo* transfection the transfection mixture was injected directly into the cardiac or skeletal muscle of animals.

Epicardial lineage tracing using modRNA gel. The Cre modRNA gel, with a mixture of Cre modRNA (10 µl of modRNA at 20 µg/µl)), lipofectamine (30 µl), and 0.05% polyacrylic acid (10 µl; Sigma), was painted on the surface of the Rosa26 (R26)^{mTmG} hearts 2 weeks before LAD ligation and injection of VEGF-A or Luc modRNA. VEGF-A– or Luc modRNA–treated hearts were assessed for expression of GFP and different myocardial markers to examine the cell fate of the EPDC derivatives 7 d after myocardial infarction.

Mice. Wt1$^{GFPCre/+}$, Wt1^{CreERT2}, R26^{fsLacZ} and R26^{mTmG} alleles have been described previously[15–17,43,49]. Genetically engineered mice were in a mixed C57BL6/CFW background and both male and female mice were used. Tamoxifen-free base (Tam) was dissolved in sunflower seed oil at 12 mg/ml by sonication. 0.12 mg/g body weight Tam was administered to adult mice twice weekly for 3 weeks to induce CreERT2-mediated recombination. One week after completion of Tam dosing (to allow Tam clearance), myocardial infarction was induced by ligation of the left anterior descending coronary artery as described below. Hearts were subsequently assessed using a combination of FACS, immunofluorescence and real-time-qPCR (RT-qPCR) analyses for GFP expression and myocardial markers after 7 d. Wt1^{GFPCre} was used for isolating Wt1$^+$ progenitor cells by the Wt1-driven GFP marker. The fate of Wt1$^+$ epicardial progenitors was determined using adult-stage irreversible labeling in the Wt1$^{CreERT2/+}$::R26^{mTmG} model. Mice that were Luc modRNA–treated after Tam induction in the presence of myocardial infarction were used as controls. To examine "leaky" CreERT2 activity that might occur under stress in the absence of Tam, mice were treated with sunflower seed oil without Tam before myocardial infarction and subsequently underwent myocardial infarction and VEGF-A modRNA or control treatments in parallel with Tam-treated mice. Wild-type were CFW strain (only males). Animals were not randomized, but procedures were done with researchers blinded to genotype and treatment group. All animals that started an experimental protocol and that survived to the measurement point were included. All mice housing and handling were performed in accordance with protocols approved by Institutional Animal Care and Use Committees at Massachusetts General Hospital or Children's Hospital Boston or Harvard University.

Cell culture. Adult CFW or WT1$^{GFPCre/+}$ hearts were digested using the Neomyt Cardiomyocyte Isolation kit (Cellutron) to achieve a single-cell suspension of adult mouse cardiac cells, according to the manufacturer's instructions. Adult mouse cardiac cells were cultured in Mesenchymal Stem Cell Growth Medium (Lonza) containing 10% FBS. Primary cultures of human fetal cardiomyocytes (obtained from Advanced Bioscience Resources, Inc. at gestational age 20 weeks) were prepared from human fetal ventricles as described before[9]. Briefly, cardiomyocytes were dissociated by means of repeated (6 ×) enzymatic digestion with collagenase II solution (Life Technologies) at 37 °C. Dissociated cells were pelleted (30 g × 2 min) and plated at a density of 1×10^5 cells/cm^2 on 35-mm culture dishes with 2 ml of culture medium (3:1 DMEM: M-199 medium with 5% FCS and 10% neonatal calf serum). Pre-plating of seeded cells onto 100-mm culture dishes to remove noncardiomyocytes (for three consecutive days) yielded cultures containing ~80% cTnT heavy chain-positive cardiac myocytes. Mouse neonatal hearts were dissociated to single cells by collagenase II (Sigma) as described previously[16]. Mouse neonatal cardiomyocytes were cultured in DMEM containing 5% FBS, 10% horse serum and 1 µg/ml insulin. Rat adult cardiomyocytes were a kind gift from R. Liao, and isolation and culture methods have been described previously[50]. All cell lines were found negative for mycoplasma contamination.

The secretion of VEGF-A protein was measured using supernatant of mouse adult cardiac cells after transfection with VEGF-A modRNA or DNA or RNA using ELISA (R&D systems). Cell transfection efficiency and survival after modRNA transfection was determined as follows: 4 wells were transfected with each different concentration of modRNA GFP (with 0, 0.3, 1 or 3 µg per 10^5 cells in a well of a 6-well plate). 16 h after transfection of cardiac cells, 2 wells from each treatment were trypsinized and stained for trypan blue. The percentage of intact cells was calculated as the number of trypan blue–negative cells per treatment well/number of trypan blue–negative cells per well without any treatment *100. To determine transfection efficiency, the two remaining wells were stained for TNNT2 (red) and GFP (green), and double-positive cells were measured using ImageJ software.

Wt1-GFP$^+$ cell isolation and *in vitro* clonal assays. WT1$^+$ epicardial progenitors were isolated from the heart explants of WT1$^{GFPCre/+}$ mice 7 d after myocardial infarction. Cardiac cells (nonmyocytes) were allowed to expand from heart explant cultures. As a control, hearts from uninjured Wt1$^{GFPCre/+}$ or Wt1$^{CreERT2/+}$::R26^{mTmG} mice treated either with vehicle or hVEGF-A modRNA were also analyzed. After 1–2 weeks, cells were FACS sorted (FACS Aria III) for GFP$^+$ cells (WT1$^+$). Single cells or pooled cells of WT1$^+$ epicardial progenitors were plated in a fibronectin-coated (5 ng/ml for 2 h at 37 °C) 96-well plate or 1 well of a 12-well plate, respectively. Cell proliferation of the WT1$^+$ epicardial progenitors was assessed in the presence or absence of VEGF-A (50 ng/ml) or different KDR inhibitors, including SU5614 or PTK787 (10 nM/l) or DMSO control at different time points (4, 8 and 14 d). Media were changed every 3 d. Calibration curve of DMSO and KDR inhibitors indicate that the optimal range (ratio of cell death of vehicle treatment (DMSO control) to KDR inhibitors) of using these inhibitors *in vitro* is 4–10 nmol/l. Cells were counted using an automated cell counter (Invitrogen).

For clonal assays, epicardial explants from Wt1$^{GFPCre/+}$ myocardial infarction mice were cultured as described[17]. Explant outgrowths were then dissociated and WT1$^+$ epicardial cells were FACS sorted. Single sorted cells were deposited into fibronectin-coated 96-well plates and clonally expanded in the presence or absence of VEGF-A (100 µg/ml) for 7–14 d before examination for their cell fate change *in vitro*. For FACS analyses, sorted cells were incubated with fluorochrome-conjugated primary antibodies at 4 °C for 30 min followed by three washes with PBS/2% FBS and resuspended in Hank's balanced salt solution. Flow cytometric analyses were done using a BD FACSCanto

© 2013 Nature America, Inc. All rights reserved.

doi:10.1038/nbt.2682

analyzer. GFP$^+$ fibroblasts, cardiomyocytes, smooth muscle and endothelial cells were assessed by immunostaining and treatment-blind cell counts were done through serial sections using ImageJ software.

Immunodetection methods. Immunostaining was performed on cryosections using standard protocols with the antibodies listed in **Supplementary Table 5**. Isolectin B4 (Vector Lab) was used to stain endothelial cells in cryosections to determine capillary density. TUNEL (Roche) or Annexin V staining (eBiosciences) was done to detect apoptosis, according to the manufacturer's instructions. To examine blood vessel leakiness, a mixture of 250 µl isolectin B4 (0.5 mg/ml, Vector Lab) and 250 µl 70 kD FITC-dextran beads (50 mg/ml, Sigma) was injected into the tail vein 7 d after myocardial infarction. Hearts were removed for histological analysis 30 min after tail vein injection. Quantification of immunostaining in cardiac sections was done using the ImageJ Software. For each image, color channels (red, blue and green) were first separated into different images. After separation, the intensity of single-color signals within each image was quantified by the software. Specific structures in the images (e.g., blue ovals corresponding to DAPI-stained nuclei) were defined by intensity threshold analysis. Definition of discrete structures by the software was further refined by contour and area analysis.

Statistical analyses. Statistical significance was determined by paired *t*-test for the MRI results, Log-rank (Mantel-Cox) test for survival curves or Student's *t*-test for other experiments, with $P < 0.05$ taken as significant. Values were reported as mean ± s.e.m. Two-sided Student's *t*-test based on assumed normal distributions. Sample sizes were selected for 80% power to detect a biologically meaningful effect given our past experience with intragroup variance.

Experimental MI model. All surgical and experimental procedures with mice were done in accordance with protocols approved by Institutional Animal Care and Use Committees at Massachusetts General Hospital or Children's Hospital Boston. MI was induced in CFW, C57Bl/6 and R26fsLacZ, R26mTmG, Wt1ERT2::R26mTmG by permanent ligation of the LAD, as previously described[51]. Briefly, the left thoracic region was shaved and sterilized. After intubation, the heart was exposed through a left thoracotomy. A suture was placed to ligate the LAD. The thoracotomy and skin were sutured closed in layers. Excess air was removed from the thoracic cavity, and the mouse was removed from ventilation when normal breathing was established. In order to determine the effect of hVEGF-A modRNA in cardiovascular outcome after MI, lipofectamine vehicle, hVEGF-A modRNA (100 µg/heart) or hVEGF-A DNA (100 µg/heart) were injected into the infarct zone immediately after LAD ligation. Sham controls were the same as the MI operation but without LAD ligation. Where indicated, DMSO or VEGF receptor inhibitors (0.5 mg/mouse intraperitoneally) were administered daily from 1 d before to 7 d after MI. Inhibitors used were SU5614 (Sigma) or PTK787 (Selleckchem). In short-term survival experiments mice that were injected with VEGF-A modRNA or DNA after MI were treated twice a week with humanized anti-VEGF monoclonal antibody (Avastin, a kind gift from D.M.B.) for 4 weeks. For analysis, the peri-infarct zone near the apex was either snap-frozen for RNA isolation and subsequent real-time qPCR studies or was fixed in 4% PFA for cryosectioning and immunostaining. For Cre gel experiments, the gel was delivered through a lower intercostal space than that used for LAD ligation 2 weeks later. In all experiments, the surgeon was blinded to treatment group. To obtain a three-dimensional cast of the vasculature, a ligature was placed on the aorta and yellow MicroFil (Flow Tech, Inc.) was injected proximally to fill and opacify the coronary vasculature. Hearts were cleared by washing through an ethanol-methyl salicylate series (25% for 1 d, 50% for 1 d, 75% for 1 d, 92% for 2 d, 100% for 1 d). To examine the localization of X-gal$^+$ cells, X-gal (Fermentas) staining was done according to manufacturer's instruction. To examine the degree of fibrosis, short-axis slices of the heart were created at defined intervals from the apex to the base of the left ventricle. These slices were stained with Masson's trichrome (Leica) according to the manufacturer's instructions. In each slice, areas of fibrosis (revealed by blue staining) were measured with the UTHSCSA ImageTool software package[52]. Detection of luciferase+ cells *in vivo* using the IVIS system. Vehicle (a mixture of 75 µl RNAiMAX and 5 µl opti-MEM basal medium) or Luc modRNA (100 µg/heart) was administered intramuscularly into the left ventricle of hearts of BALB/c mice or skeletal muscle (biceps femoris) of CFW mice. Bioluminescence imaging of the injected mice was taken at different time points (3–240 h) which each unit represent p/sec/cm2/srX106 (Luc signal). To visualize Luc$^+$ cells, luciferin (150 µg/g body weight; Sigma) was injected intraperitoneally. After 10 min, mice were anesthetized with isoflurane (Abbott Laboratories), and imaged using an IVIS100 charge-coupled device imaging system for 2 min. Imaging data were analyzed and quantified with Living Image Software. The strength of the signal was indicated by the spectrum of 12 different colors. Hearts or skeletal muscles that were injected with the vehicle only served as baseline for Luc expression.

MRI. C57Bl/6 (6–8 weeks old) treated with vehicle or hVEGF-A modRNA were subjected to MRI assessment at days 1 and 21 after LAD ligation. We obtained delayed-enhancement CINE images on a 7-T Bruker Pharmascan with cardiac and respiratory gating (SA Instruments, Inc., Stony Brook, New York). Where ejection fraction was within the range of 50–60%, follow-up MRI analyses were performed on the same mice at day 21 post-MI to determine temporal changes in infarct size and cardiac function. Mice were anaesthetized with 1–2% isofluorane/air mixture. ECG, respiratory and temperature probes were placed on the mouse which was kept warmed during scans. Imaging was performed 10 to 20 min after IV injection of 0.3 mmol/kg gadolinium-diethylene triamine pentaacetic acid. A stack of short-axis slices covering the heart from the apex to the base was acquired with an ECG triggered and respiratory-gated FLASH sequence[53] with the following parameters: echo time (TE) 2.7 msec with resolution of 200 µm × 200 µm; slice thickness of 1 mm; 16 frames per R-R interval; four excitations with flip angle at 60°. Eight to ten short-axis slices were acquired from the apex to the base to cover the left ventricle. Ejection fraction was calculated as the difference in end-diastolic and end-systolic volumes, divided by the end-diastolic volume. MRI acquisition and analyses were performed blinded to treatment group.

RNA isolation and gene expression profiling. Total RNA was isolated using the RNeasy mini kit (Qiagen) and reverse transcribed using Superscript III reverse transcriptase (Invitrogen), according to the manufacturer's instructions. Real-time qPCR analyses were performed on a Mastercycler realplex 4 Sequence Detector (Eppendorf) using SYBR Green (QuantitectTM SYBR Green PCR Kit, Qiagen). Data were normalized to Gapdh or Actb expression, where appropriate (endogenous controls). Fold-changes in gene expression were determined by the ∂∂CT method and were presented relative to an internal control. PCR primer sequences are shown in **Supplementary Table 6**. To characterize GFP$^+$ progenitors, total RNA was obtained from FACS-sorted GFP$^+$ cells, isolated after collagenase digestion of the vehicle-treated or the hVEGF-A modRNA–treated hearts derived from WT1GFPCre/+ or WT1CreERT2/+ :: R26mTmG mice 7 d post MI using a FACSAria III cell sorter. To examine the expression level of Wt1 among different tissues, bone marrow, spleen, heart and blood cells were isolated from CFW mice injected with VEGF-A modRNA (100 µg) or vehicle.

Myotube differentiation and transfection. Skeletal muscle myotubes were differentiated from primary mouse satellite cells. Satellite cell isolation was performed as previously described[54,55]. Briefly, myofiber-associated (MFA) cells were prepared from intact skeletal muscles (Extensor digitorum longus, gastrocnemius, quadriceps, soleus, tibialis anterior, triceps brachii, abdominal) by digesting the muscles with collagenase type II and then dispase enzymes. MFA cells were stained for isolation of CD45- Sca-1- Mac-1- CXCR4$^+$ β1-integrin$^+$ cells by FACS. Isolated cells were seeded on collagen/laminin-coated plates in F10 medium (Gibco) containing 20% horse serum (Atlanta Biologics), 1% penicillin-streptomycin (Invitrogen) and 1% glutamax (Invitrogen). 5 ng/ml bFGF (Sigma) was added to the media daily and cells were expanded for 5 d. On day 5, cells were harvested and equal numbers (8,000 cells) were replated in each well of a 96-well plate in growth media. Media was changed to DMEM (Gibco), containing 2% horse serum (Atlanta Biologics) and 1% penicillin-streptomycin (myotube differentiation media) after 12 h. Cells were transfected with modified RNA after 3 d in differentiation media. Myotubes were transfected with 0, 0.3, 1 or 3 µg of GFP-modified RNA using lipofectamine RNAiMax transfection reagent (Invitrogen) according to the manufacturer's instructions. Transfection reagent was changed to myotube differentiation media after 6 h and cells were fixed 16 h after transfection. Transfected myotubes

© 2013 Nature America, Inc. All rights reserved.

were stained for skeletal muscle myosin heavy chain (Primary antibody: anti-skeletal myosin type II (fast- twitch) 1:200 and anti-skeletal myosin type I (slow-twitch) 1:100, Sigma. Secondary: goat anti-mouse IgG Alexa-555 conjugate (Molecular Probes) 1:250), 10 μg/ml Hoechst (Invitrogen) and rabbit anti-GFP Alexa-488 1:200 (Invitrogen). Pictures were taken from the whole well using the Celigo cytometer (Cyntellect) under blue, red and green channels. Cell viability was measured by quantifying the total number of nuclei in the transfected wells 16 h after transfection and normalizing them to the total number of nuclei in the nontransfected wells. Total number of nuclei in the whole wells was quantified using a modified ImageJ macro.

49. Soriano, P. Generalized lacZ expression with the ROSA26 Cre reporter strain. *Nat. Genet.* **21**, 70–71 (1999).
50. Liao, R. & Jain, M. Isolation, culture, and functional analysis of adult mouse cardiomyocytes. *Methods Mol. Med.* **139**, 251–262 (2007).
51. Tarnavski, O. *et al.* Mouse cardiac surgery: comprehensive techniques for the generation of mouse models of human diseases and their application for genomic studies. *Physiol. Genomics* **16**, 349–360 (2004).
52. Takagawa, J. *et al.* Myocardial infarct size measurement in the mouse chronic infarction model: comparison of area- and length-based approaches. *J. Appl. Physiol.* **102**, 2104–2111 (2007).
53. Lee, W.W. *et al.* PET/MRI of inflammation in myocardial infarction. *J. Am. Coll. Cardiol.* **59**, 153–163 (2012).
54. Cerletti, M. *et al.* Highly efficient, functional engraftment of skeletal muscle stem cells in dystrophic muscles. *Cell* **134**, 37–47 (2008).
55. Sherwood, R.I. *et al.* Isolation of adult mouse myogenic progenitors: functional heterogeneity of cells within and engrafting skeletal muscle. *Cell* **119**, 543–554 (2004).

© 2013 Nature America, Inc. All rights reserved.

doi:10.1038/nbt.2682